SPECTRAL ANALYSIS USING CCDS

D. D. Buss,* R. W. Brodersen,** C. R. Hewes* and M. de Wit*

ABSTRACT

Charge-coupled devices (CCDs) are ideally suited for performing n sampled-data transversal filtering operations in the analog domain. Two algorithms have been identified for performing spectral analysis in which the bulk of the computation can be performed in a CCD transversal filter; the chirp z-transform and the prime transform. CCD implementation of both these transform algorithms is presented together with performance data and applications.

I. INTRODUCTION

From the standpoint of minimizing the number of digital operations required to perform the discrete Fourier transform (DFT), the fast Fourier transform (FFT) algorithm is optimum. (ref. 1) However, in determining the optimum algorithm for implementation with analog charge-coupled devices (CCDs), a whole new set of ground rules exists. In this case, it is no longer important to minimize multiplications, because CCD transversal filters can be built which perform a large number of multiplications simultaneously in real time. (ref. 2) Consequently, for CCD implementation, algorithms should be selected in which the bulk of the computation is performed by a transversal filter. Two such algorithms have been identified for cost-effective CCD implementation; the chirp z-transform (ref. 3) (CZT) and the prime transform. (ref. 4) CCD implementation of both types of transform are discussed in this paper.

In Section II, the CZT algorithm is discussed, and results are presented for a system which performs a 500-point power density spectrum. The performance of the CCD CZT is compared with that of a digital FFT. In Section III, the prime transform is discussed, and results are presented on a 31-point, CCD, prime transform unit. In Section IV, applications of the CCD CZT and the CCD prime transform are discussed.

II. CCD CHIRP Z-TRANSFORM

The CZT gets its name from the fact that it can be implemented by (1) premultiplying the time signal with a chirp (linear FM) waveform, (2) filtering in a chirp convolution filter, and (3) postmultiplying with a chirp waveform. When implemented digitally, the CZT has no clear cut advantages over the conventional FFT algorithm. (ref. 3) However, the CZT lends itself naturally to implementation with CCD transversal filters. (ref. 5, 6, 7, 8)

Mathematical Derivation

The DFT of the N-point sequence f_n, n=0, N-1 is defined by

$$F_k = \sum_{n=0}^{N-1} f_n e^{-i2\pi nk/N} \qquad (1)$$

*Texas Instruments Incorporated, Dallas, Texas
**University of California, Berkeley.

Making the substitution

$$2nk = k^2 + n^2 - (k - n)^2 \tag{2}$$

Equation (1) becomes

$$F_k = e^{-i\pi k^2/N} \sum_{n=0}^{N-1} (f_n e^{-i\pi n^2/N}) \, e^{i\pi(k-n)^2/N}. \tag{3}$$

This equation has been factored to emphasize the three operations which make up the CZT algorithm. It is illustrated in Figure 1. In many spectral analysis applications, the power density spectrum $|F_k|^2$ is required.

$$|F_k|^2 = \left| \sum_{n=0}^{N-1} (f_n e^{-i\pi n^2/N}) \, e^{i\pi(k-n)^2/N} \right|^2 \tag{4}$$

in which case the post multiplication of Figure 1 can be eliminated.

Equation (3) or Equation (4) can be implemented using CCD filters of length 2N-1 (ref. 7, 9). However, for many spectral analysis applications, the sliding CZT can be used which greatly simplifies the CCD electronics. The sliding DFT is defined by the relation

$$F_k^s = \sum_{n=k}^{k+N-1} f_n e^{-i2\pi nk/N} \tag{5}$$

and gives rise to the power density spectrum

$$|F_k^s|^2 = \left| \sum_{n=0}^{N-1} (f_{n+k} e^{-i\pi n^2/N}) \, e^{i\pi(k-n)^2/N} \right|^2 \tag{6}$$

Comparison of Equation (6) with Equation (4) indicates that the sliding CZT differs from the conventional CZT in that the sliding CZT indexes the data each time a spectral component is calculated. For a periodic waveform, indexing results in a phase factor which does not affect the result, and for a stationary random signal, the time record is different for each spectral component, but stationarity insures that the result is unaffected. For these two classes of signal the sliding CZT gives the same result as the conventional CZT. Figure 2 gives a pictorial comparison between the conventional CZT and the sliding CZT for the simple case of a 3-point transform. With the conventional CZT, all three Fourier coefficients F_0, F_1, F_2 are calculated using the first three time samples f_0, f_1, f_2. These coefficients are being calculated by the filter during the next three clock periods, so that time samples f_3, f_4, f_5 must be blanked. Then the cycle repeats as shown in Figure 2a. Using the sliding CZT, F_0^s is calculated on the sample record f_0, f_1, f_2 as before, but F_1^s is calculated on the sample record f_1, f_2, f_3, F_2^s on the record f_2, f_3, f_4 and the next F_0^s computation is made on the sample record f_3, f_4, f_5. The sample record is continually updated by replacing the oldest sample with a new one. The above description shows that N Fourier coefficients are obtained for N time samples (100% duty cycle).

The advantages of the sliding CZT are: (1) For an N-point transform, N-stage filters are required which chirp through a bandwidth f_c($-f_c/2$ to $+f_c/2$ for example). (2) No blanking is required. The filters operate with 100% duty cycle; i.e., one spectral component out for each time sample in. (3) Windowing can be achieved by weighting the chirp impulse response of

the filter with the desired window function. (4) The degradation due to imperfect charge transfer efficiency (CTE) is less for the sliding CZT than for the conventional CZT.

Performance of the 500-Point CCD CZT

The block diagram for obtaining the spectral density using the sliding CZT is shown in Figure 3. The rectangles represent CCD filters having impulse responses $w_n \cdot \cos\pi n^2/N$ and $w_n \cdot \sin\pi n^2/N$, $-N/2<n<N/2-1$. This system has been implemented using 500-stage CCD filters. If a windowed transform is required, the desired window function w_n is coded into the photomask[1]. Systems have been demonstrated without windowing and with Hamming windowing[7].

The experimental implementation of Figure 3 utilized two CCD ICs each containing two 500-stage filters. The premultiply chirps were stored with 8-bit precision in ROMs. Multiplication was performed in discrete multiplying digital to analog converters (MDACs), and the squaring operation was performed in bipolar analog multipliers. This experimental demonstration required 33 IC packages in addition to the two CCD packages and 16 discrete MOSFETs.

The operation of this system is illustrated in Figures 4 and 5. Figure 4 shows the response of the system clocked at 20 kHz to sinusoidal input signals. Figure 5 shows the response of the system clocked at 25 kHz to a 200 Hz square wave. The output spectrum shows odd harmonics which decrease in amplitude approximately as $1/n^2$. The effect of imperfect CTE is visible in Figure 5c as indicated by the arrow.

The system of Figure 3 is limited in dynamic range by the squaring amplifiers, which are implemented with analog multipliers. The multipliers have output dynamic range of approximately 80 dB, thereby limiting the input dynamic range to only 40 dB. The overall system up to the squaring multipliers has approximately 70 dB dynamic range, so the squaring multipliers are the weak link that limits dynamic range. To circumvent this problem, an improved magnitude circuit was implemented using bipolar amplifiers, and the output was applied to a log amplifier. The dynamic range improvement is illustrated in Figure 6. In the top photograph the maximum signal is applied to a CZT unit with Hamming windowing. With the peak at 0 dB the sidelobes are at -40 dB. In the middle photograph the input sinusoid has been attenuated by 20 dB, and in the bottom photograph it has been attenuated by 40 dB. The noise level in the bottom photograph is around -60 dB. This illustrates clearly that the CCD CZT is capable of 60 dB dynamic range.

Accuracy Comparison with the Digital FFT

The sources of error in a CCD CZT are (1) thermal noise, (2) quantization of the pre- and postmultiply chirp waveforms, (3) weighting coefficient error in the CCD transversal filters, and (4) CTE. When the criterion of rms error to rms signal is applied, imperfect CTE generates large errors, because the errors add coherently. Because of this fact, however, CTE effects can be treated as a resolution degradation and not as "random" error.

Thermal noise is analogous to input quantization in a digital FFT because it generates an error which is independent of signal size. Assuming the rms noise referred to the input is 60 dB below the maximum peak signal, the equivalent quantization accuracy is 8 bits plus sign. At higher signal levels thermal noise, like input quantization noise in a digital FFT, is dominated by signal dependent errors.

Errors which result from the 8-bit quantization of the chirp signals dominate the rms error of the 500-point CZT and give rise to an rms error to rms signal of about .003[9].

Weighting coefficient error arises from a number of sources, but let us assume as a model, that the placement of the gap in the split electrodes is quantized in steps of δ during photomask fabrication. δ can be made as small as 10 μin, and the channel width W is typically 5 mil giving $\delta/W = .002$. This is equivalent to quantizing the weighting coefficients to 8 bits plus sign and is analogous to twiddle factor quantization in the FFT. The rms error to rms signal which would result for a 500-point CCD CZT is on the order of .0008.[9]

The two error sources discussed above are independent of the number of points N in the transform and are indicated by the dashed line in Figure 7. Also shown in Figure 7 are the results of a computer simulation of error using randomly generated errors.

For comparison with the digital FFT, a block floating point truncation algorithm is assumed.

The most important source of error in this type of FFT is usually overflow and round-off of data words during butterfly computation. If the data words are carried with "b" bits plus sign, an upper bound on error in a block floating point machine can be determined assuming overflow occurs at every stage. The result is[10]

$$\Delta_B = .3\sqrt{8}\, N^{\frac{1}{2}}\, 2^{-b} \quad . \tag{7}$$

If the twiddle factors are quantized to the same accuracy as the data words, Δ_B dominates FFT error. Although Equation (7) does not contain the input signal size explicitly. Δ_B does scale in a general way with signal because for smaller signals, overflow does not occur at every stage. The dependence of Δ_B on the length of the transform indicates that higher accuracy (larger b) is required for longer transforms.

For fixed b, Δ_B increases like $\sqrt{N}$, and it is plotted in Figure 7 for the case b = 13. Figure 7 shows that a 512-point, block floating point FFT with 14-bit internal arithmetic is comparable in terms of rms error to the CCD CZT.

The performance limitations of the CCD CZT and the digital FFT are summarized in Table 1.

III. CCD PRIME TRANSFORM

The prime number algorithm[4,11] is based on a number of theoretic property of prime numbers and the modulo arithmetic implied in the Fourier weighting coefficients $\exp(i2\pi k/N)$. The property that is used is the existence of primitive roots of the prime. If the number of points N in the DFT is a prime P, then there are one or more primitive roots g. These have the property that the set of numbers

$$g^k \pmod{P} \qquad \text{for } k = 1, 2, \ldots, P-1 \tag{8}$$

is just the set (1,2,..., P-1) rearranged. Any integer M (mod P) is equal to one, and only one, g^k. The exponent k then is called the index of M, (Ind M). IndM is modulo arithmetic is the analog of logarithms in normal arithmetic. We have that

$$\text{Ind}\,(M \cdot K) = \text{Ind}\, M + \text{Ind}\, K. \tag{9}$$

This property is used in the DFT by calculating the coefficient $F\, g^k \pmod{P}$ and ordering the data according to the sequence $g^n \pmod{P}$ for n=1, 2, ..., P-1. With (mod P) suppressed in the notation we have then[4]:

$$F(g^k) - f(0) = \sum_{n=1}^{P-1} f(g^n)\, W(g^n \cdot g^k) \quad , \tag{10}$$

$$= \sum_{n=1}^{P-1} F(g^n)\, W(g^{n+k}) \quad , \tag{11}$$

Equation (11) is in the convolution form and can be implemented with a CCD transversal filter.[11]

The prime transform algorithm is implemented in 3 steps as indicated in figure 8; (1) permutation of the input data, (2) transversal filtering and (3) permutation of the output Fourier coefficients. The advantages of the prime transform over the CZT are (1) the multipliers are replaced by permuting memories. (This may or may not be an advantage depending upon the speed and dynamic range required) and (2) for a real input, only two filters are required instead of the four shown in Figure 3. The disadvantages are (1) the zero order Fourier coefficient (dc term) must be computed separately, (2) imperfect CTE does not result in a simple degradation in resolution as it does in the CZT and (3) the sliding DFT cannot be implemented with the prime transform. The CCD prime transform may be important for application in which (1) the phase of the DFT is required thus ruling out the sliding CZT and (2) high speed and high dynamic range make on-chip multipliers difficult to implement.

The operation of a CCD transversal filter designed for a 31-point discrete cosine transform is illustrated in Figure 9. The filter is clocked at 5 MHz, and one Fourier coefficient is generated every 200 nsec. The input is a symmetric 161 kHz square wave, and the permuted input is simulated with a digital word generator. The output is displayed in permuted form and odd harmonics 1 through 11 are indicated on the photograph.

Permutation of the input and output waveforms can be performed in analog random access memories.[12] However, preliminary operation at 1.7 MHz has been limited by fixed pattern noise in the permuting memory to only 30 dB.

V. APPLICATIONS

For a given spectral analysis application to be considered as a candidate for CCD CZT or prime transform implementation it must satisfy two criteria: (1) It must be of modest performance which lies within the CCD performance limitations and (2) it must be required in sufficiently high volume that low cost is a dominant design specification. These two criteria rule out a large class of applications. However, there have been identified, several applications of great importance which do satisfy both of the above criteria.

- Video bandwidth reduction[13]
- Speech processing[14]
- Doppler processing in MTI radar[15]
- Sonar spectral analysis
- Remote surveillance
- Image enhancement

The CCD CZT and prime transform are not expected to make the digital FFT obsolete in signal processing systems. However, for those spectral analysis applications which fulfill the twin requirements of modest performance and high volume, tremendous cost advantages can be gained with CCD implementation. More applications will certainly emerge, but in the meantime, the potential cost impact in the application areas already

identified guarantees the importance of CCDs in spectral analysis applications of the future.

ACKNOWLEDGEMENT

Development of the CCD CZT at Texas Instruments has been sponsored by the Army Electronics Command (Robert Sproat, contract monitor), by the Defense Advanced Research Projects Agency/Naval Undersea Center (Robert Means, contract monitor), and by the National Aeronautics and Space Administration (Harry Benz, contract monitor).

REFERENCES

1. For a discussion of the FFT, see L. R. Rabiner and B. Gold, Theory and Application of Digital Signal Processing, Prentice-Hall, 1975, Section 6.
2. For a discussion of CCD transversal filters see C. H. Séquin and M. F. Tompsett, Charge Transfer Devices, Academic Press, 1975, Section VI-D.
3. L. R. Rabiner, R. W. Schafer, and C. M. Rader, "The Chirp Z-Transform Algorithm," IEEE Trans. on Audio and Electroacoustics, AU-17, pp. 86-92, June 1969.
4. C. M. Rader, "Discrete Fourier Transforms when the Number of Data Samples is Prime," Proc. IEEE, 56, pp 1107-1108, June 1968.
5. H. J. Whitehouse, J. M. Speiser and R. W. Means, "High Speed Serial Access Linear Transform Implementations," presented at the All Applications Digital Computer Symposium, Orlando, Florida, 23-25 January 1973, NUC TN 1926.
6. R. W. Means, D. D. Buss, and H. J. Whitehouse, "Real Time Discrete Fourier Transforms Using Charge Transfer Devies," Proc. CCD Applications Conference, San Diego, pp. 127-139, September 1973.
7. R. W. Brodersen, C. R. Hewes and D. D. Buss, "A 500-Stage CCD Transversal Filter for Spectral Analysis," IEEE J. Solid-State Circuits, SC-11, pp 75-84, February 1976.
8. G. J. Mayer, "The Chirp Z-Transform - A CCD Implementation," RCA Review, 36, pp 759-773, December 1975.
9. D. D. Buss, R. L. Veenkant, R. W. Brodersen and C. R. Hewes, "Comparison Between the CCD CZT and the Digital FFT," CCD '75 Proceedings, pp 267-281, San Diego, October 1975.
10. P. D. Welch, "A Fixed-Point Fast Fourier Transform Error Analysis," IEEE Trans. on Audio Electroacoustic, AU-17, pp 151-157, June 1969.
11. H. J. Whitehouse, R. W. Means and J. M. Speiser, "Signal Processing Architectures Using Transversal Filter Technology," IEEE Advanced Solid-State Components for Signal Processing, pp 5-29, IEEE International Symposium on Circuits and Systems, Newton, Mass., April 1975.
12. To be published
13. R. W. Means, H. J. Whitehouse and J. M. Speiser, "Television Encoding Using a Hybrid Discrete Cosine Transform and a Differential Pulse Code Modulator in Real Time," 1974 National Telecommunications Conference Record, pp 69-74, San Diego, December 1974.
14. R. W. Schafer and L. R. Rabiner, "Digital Representations of Speech Signals," Proc. of the IEEE, 63, pp 662-677, April 1975.
15. W. H. Bailey, D. D. Buss, L. R. Hite and M. M. Whatley, "Radar Video Processing Using the CCD Chirp Z-Transform," CCD '75 Proceedings, pp 283-290, San Diego, October 1975.

FIGURE CAPTIONS

Figure 1. Schematic of the CZT algorithm.

Figure 2. Comparison between the conventional CZT and the sliding CZT for the case of a 3-point transform.

Figure 3. An implementation of the CZT algorithm using real components. The power density spectrum $|F_k|^2$ is computed for a real input.

Figure 4. Power density spectra for three sinewaves obtained using the 500-point sliding CCD CZT at a sample rate of 20 kHz.

Figure 5. 500-point power spectrum of a 200 Hz square wave for a sample rate of 25 kHz. (a) Input waveform; (b) power spectrum output showing the first nine harmonics; (c) the output amplified by 10, which shows a small trailing pulse due to transfer inefficiency (pointed out by the arrow); and (d) the 11th through 19th harmonics amplified by 100.

Figure 6. Output of an apodized CZT unit when a single frequency sinusoid is applied to the input. The top photograph shows -40 dB sidelobes when the maximum signal amplitude is applied. The center and bottom photographs show the output when the input is attenuated by 20 dB and 40 dB, respectively. The noise level in the bottom photograph is approximately -60 dB.

Figure 7. Error comparison between a CCD CZT and a digital FFT implemented using 13 bits plus sign. The CCD CZT is limited by the quantization of multiply chirps to 7 bits plus sign. The points represent computer simulation for the CCD CZT.

Figure 8. Block diagram of the prime transform implemented with CCDs.

Figure 9. A 31-point prime cosine transform operating at 5 MHz clock rate. The input is a signal cycle of a square wave of frequency 161 kHz. The output is shown in permuted form. The odd harmonics of the square wave are identified.

TABLE 1

CCD CZT PERFORMANCE LIMITATION

Parameter	Limitation	Value
Transform Length	Imperfect CTE Chip Size	1000
Time Record	Leakage Current	1 sec
Speed	Analog Circuitry	5 MHz
Accuracy	Premultiply Quantization; Weighting Coefficient Error	13 - Bit Equivalent FFT
Resolution	Imperfect CTE	5% Degradation

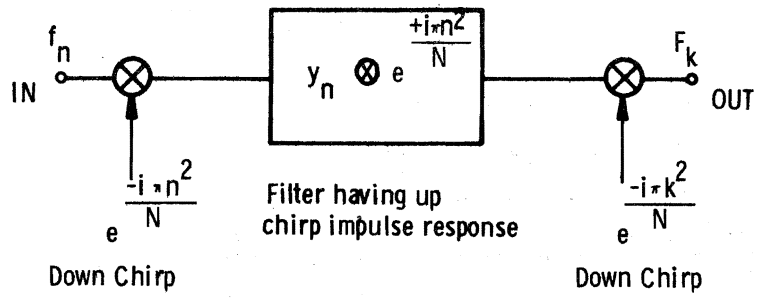

Figure 1

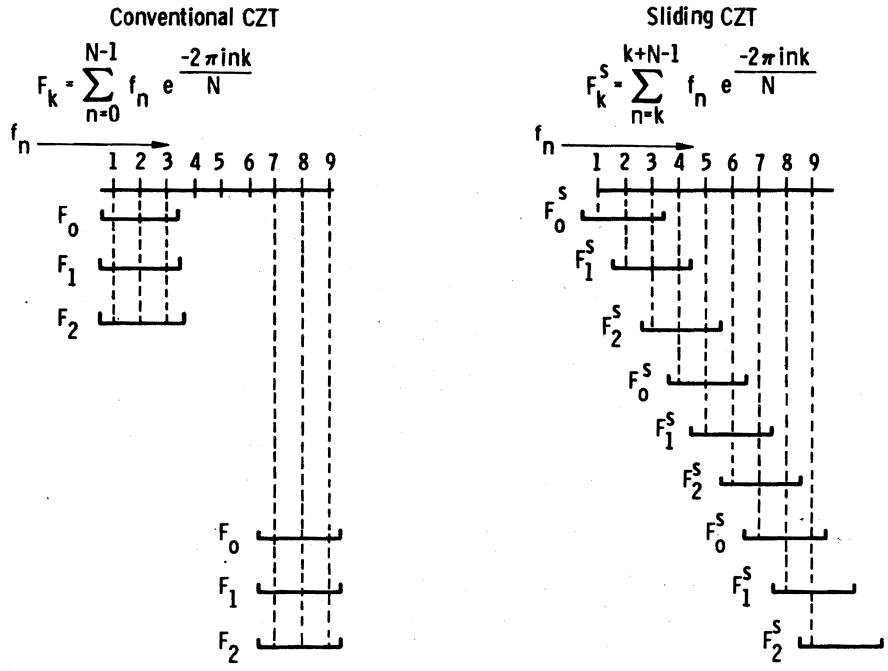

Figure 2

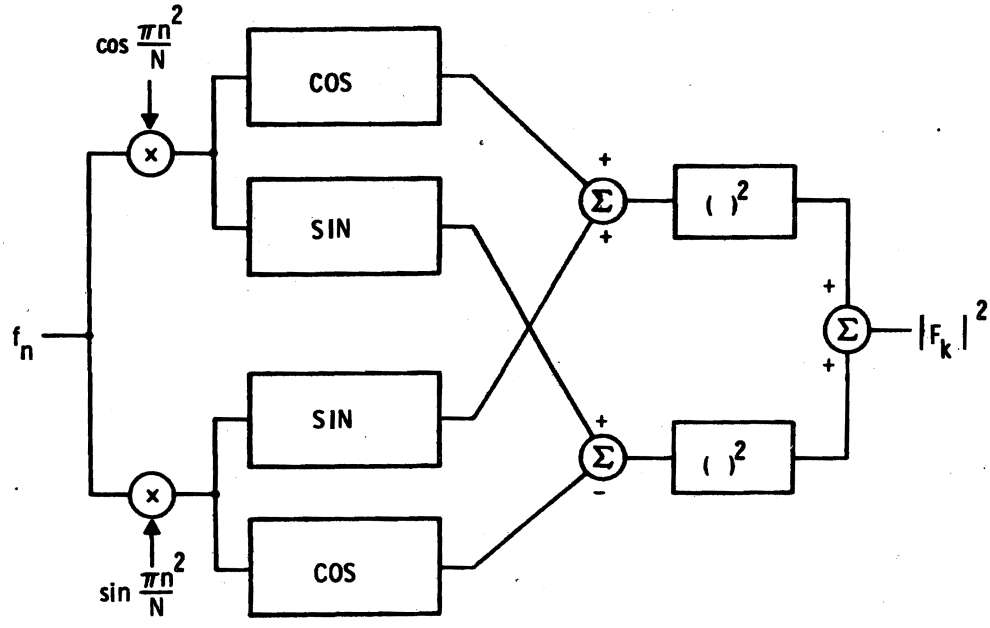

Figure 3

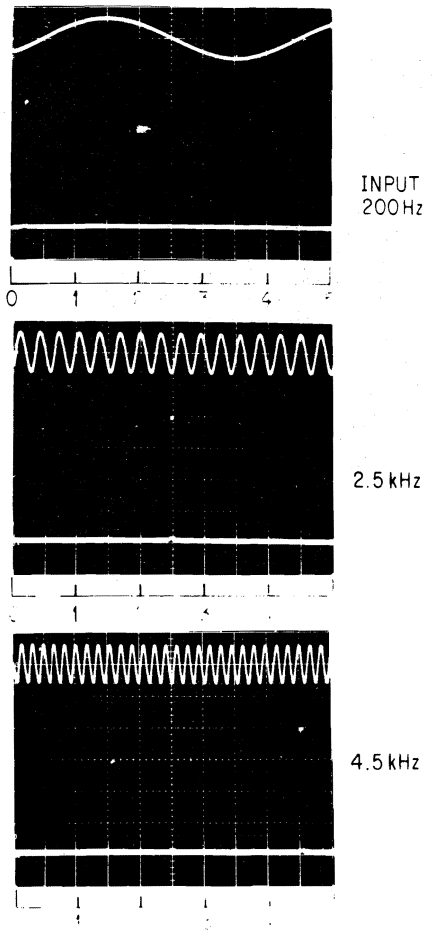

Figure 4

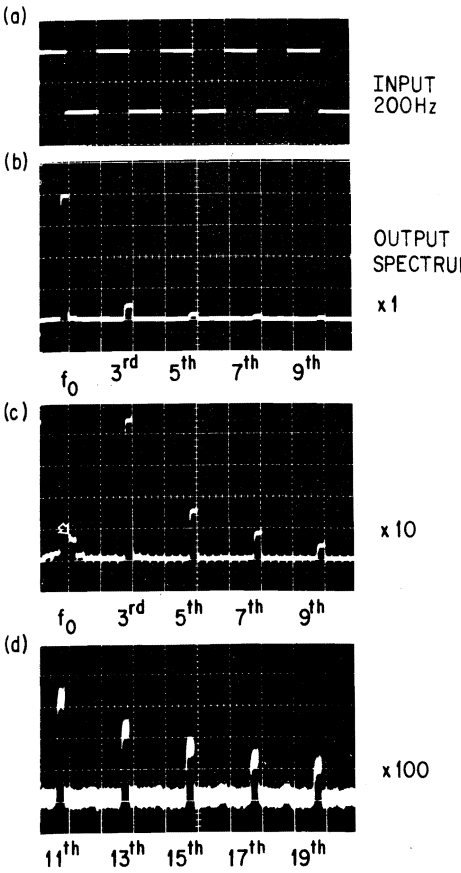

Figure 5

DYNAMIC RANGE OF CCD - CZT

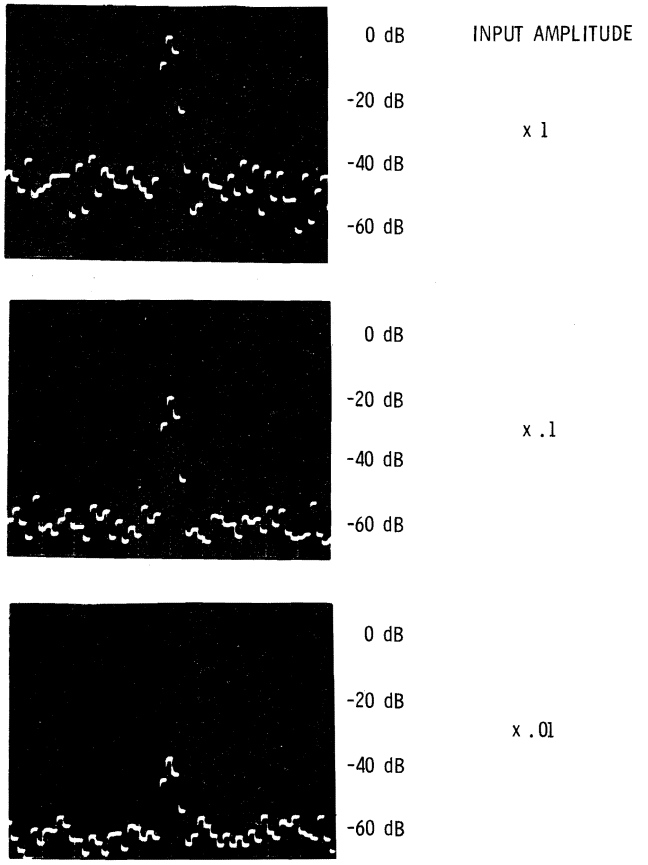

Figure 6

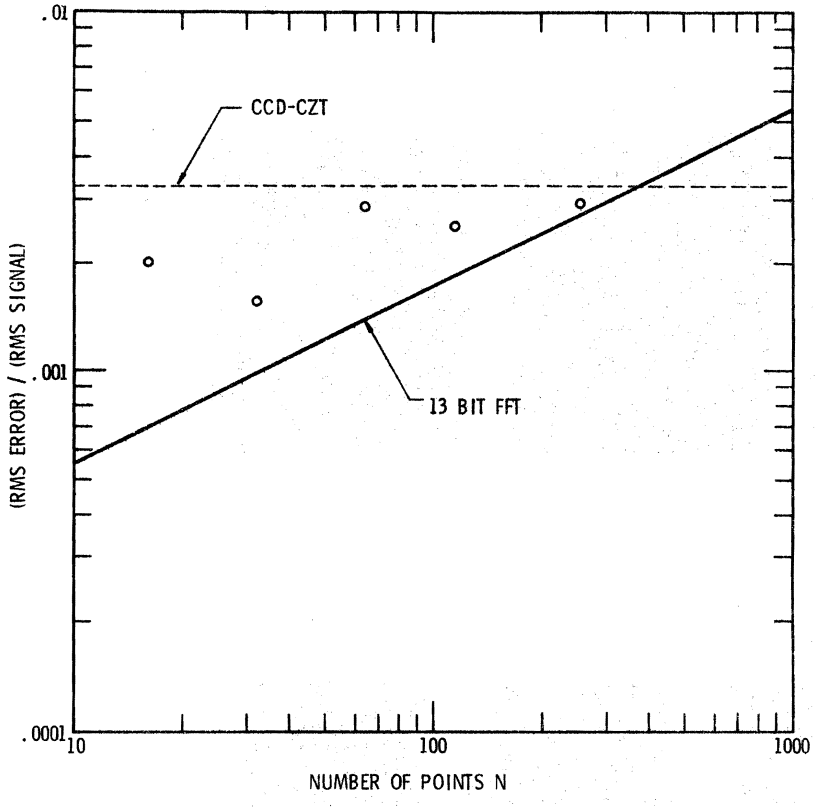

Figure 7

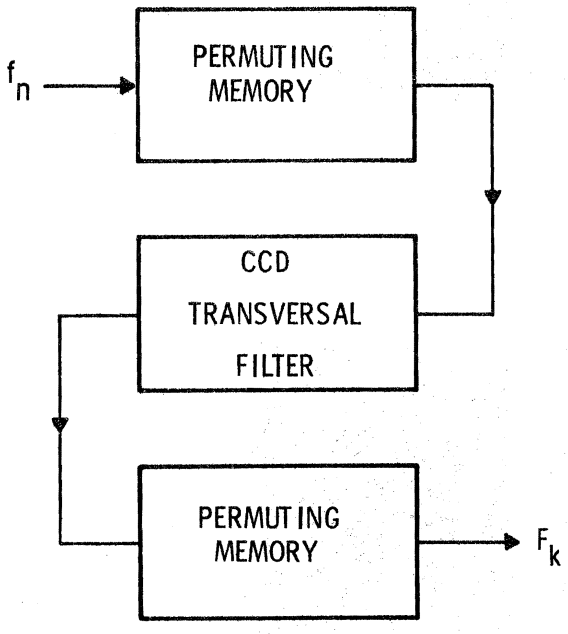

Figure 8

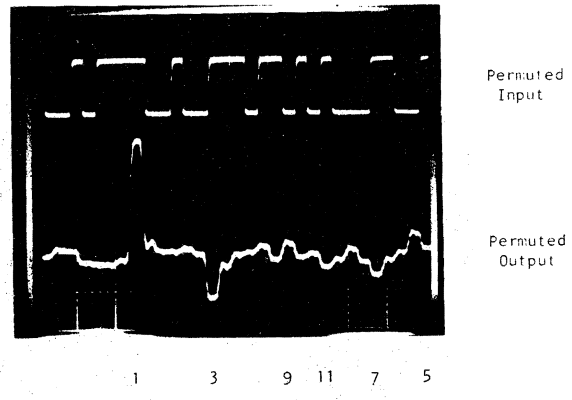

Figure 9